

Crystallization Behavior and Mechanical Properties of Hyperbranched Polyesters in Toner Polymer Blends

Alan Toman[▲], Chris Provost and Jennifer Polley

Reichhold Inc., Research Triangle Park, North Carolina, USA

Hyperbranched polymers with crystalline surface groups were synthesized and their crystallization behavior in the presence of primary toner polymers was investigated. In contrast to linear crystalline polymers, their crystallization is relatively unaffected by the presence or chemical structure of the primary toner polymer. They do not affect the glass transition temperature of the primary toner polymer and the polymer blends have lower storage modulus at low temperature but increased storage modulus at elevated temperature.

Journal of Imaging Science and Technology 49: 641–645 (2005)

Introduction

In typical toner applications, heat roller fixing is used to fuse toner particles onto the transfer paper. The transfer paper is passed through a combination of a heated roller and a pressure roller. If the temperature of the heating roller is too low, the surface of the particles in contact with the paper will not soften and no adhesive force will be generated. This results in transfer of the toner only to the heated roller and is referred to as cold offset. If the temperature of the heated roller is too high, the internal cohesive force of the toner becomes less than the adhesive forces to the heated roller and paper. This results in rupture of the toner layer and some of the toner is transferred onto the heated roller. This behavior is referred to as hot offset.

Crystalline polymers have been used in toners to lower the temperature at which cold offset occurs.^{1–4} They function by reducing the storage modulus and viscosity of the toner at low temperature,⁵ and consequently improve adhesion to the transfer paper. For minimizing the cold offset fusing temperature, the melt point T_m of the crystalline polymer should be as low as possible.¹ However, crystalline polymers can also reduce the storage modulus of the toner at higher temperature. This can result in a lowering of the temperature at which hot offset occurs.

Using crystalline polymers can lead to poor physical stability of the toner and poor block resistance of printed

sheets. Crystallization involves the orderly arrangement of polymer chains. With a pure crystalline polymer the influence of chain diffusion is negligible. When blended with a primary toner polymer, its crystallization rate can be significantly lowered. This is due to the lower concentration of crystalline polymer and chain entanglements with the primary toner polymer which results in slower chain diffusion. The polymer chains that are not incorporated into a crystalline domain cause a plasticization effect by lowering of the glass transition temperature T_g of the toner. In addition, crystallization typically occurs only in the temperature range between the T_m and T_g of the formulated toner. Since the T_g of the toner is predominately controlled by the primary toner polymer this requires using a crystalline polymer with a melt point that is significantly higher than the T_g of the primary toner polymer.

The size of the dispersed phase of the crystalline polymer can influence toner properties.⁴ Decreasing the domain size imparts a lower minimum fusing temperature, but the physical stability of the toner is reduced.⁶ This is also caused by a lower crystallization rate from the diffusion controlled crystallization process. Therefore, differences in toner processing conditions can result in variable product performance.

Hyperbranched Polymers

Dendrimers and hyperbranched polymers belong to a unique class of polymers having properties that differ significantly from linear or lightly branched polymers. These polymers are highly branched and have a three dimensional, tree-like structure. They are globular or approximately spherical in shape and have a compact size even with high molecular weight. Dendrimers have a branch point at every repeat unit in the polymer while hyperbranched polymers can contain some linear segments. Both of these polymer types have a high number and density of functional groups that are primarily located at the periphery or surface of the molecule. Their

Original manuscript received January 31, 2005

▲ IS&T Member

Corresponding Author: A. Toman, Alan.toman@reichhold.com

©2005, IS&T—The Society for Imaging Science and Technology

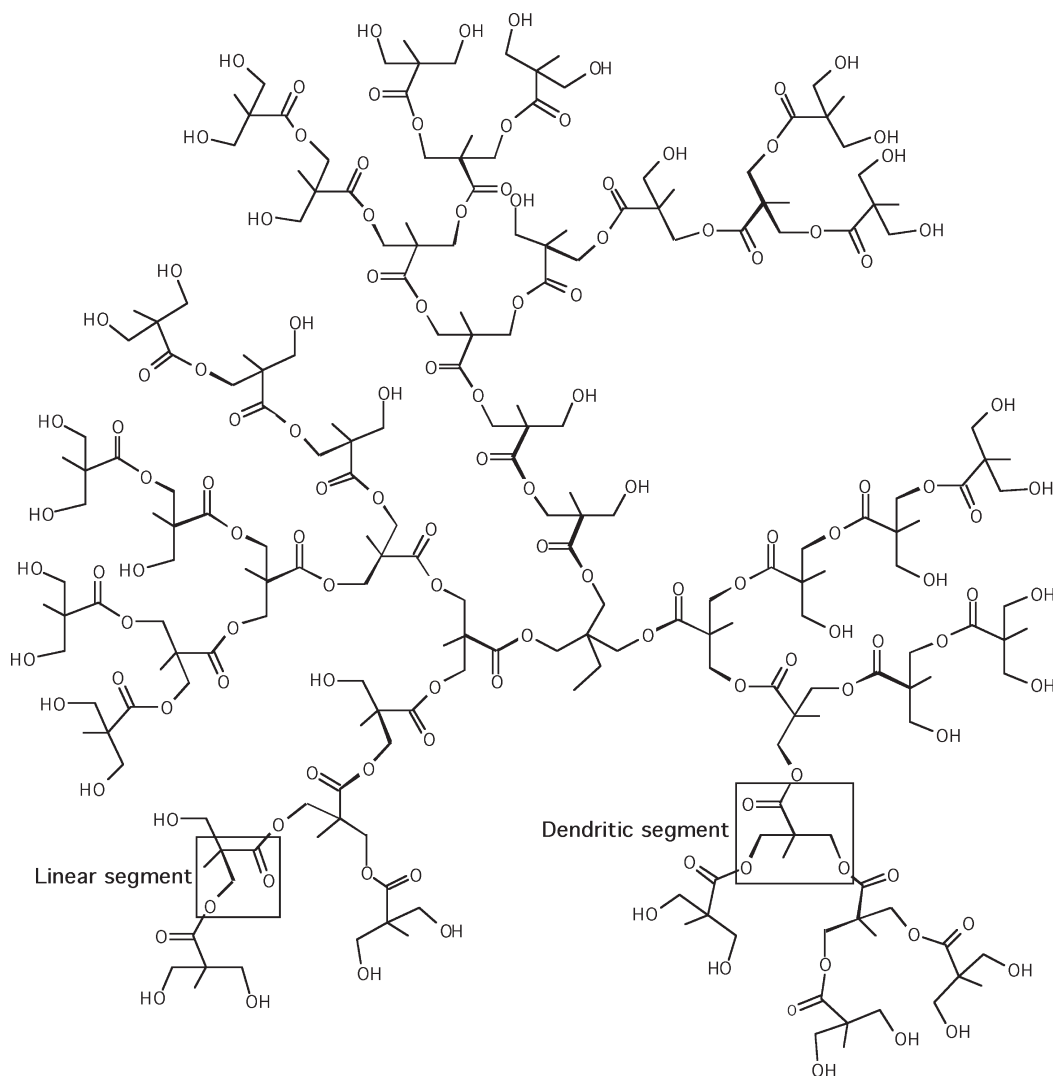


Figure 1. Chemical structure of hyperbranched polyester.

properties are predominately controlled by the composition of these surface groups. An example of a hyperbranched polymer is shown in Fig. 1.

Due to the high level of branching, hyperbranched polymers are usually amorphous. Attachment of appropriate groups at the surface of the molecule provides the crystalline structure. For the polymer shown in Fig. 1, esterification of the hydroxyl groups with a long chain carboxylic acid containing at least 14 carbons gives a polymer with a melt point above room temperature. Hyperbranched polymers that have crystalline surface groups have been found to crystallize by an intramolecular mechanism⁷ and therefore should have a crystallization rate is not diffusion controlled. This occurs when the molecular weight of the polymer is high and the chain length of the surface group is sufficiently long.

Experimental

Materials

Hyperbranched polymers were synthesized from the reaction of trimethylolpropane and dimethylolpropionic acid.⁸ The hydroxyl groups of this intermediate were then esterified with various aliphatic carboxylic acids. The influence of the carboxylic acid chain length on the melt point of the final polymer is shown in Fig. 2.

When the hyperbranched intermediate is reacted with stearic acid (C_{18}) a polymer is obtained that has a melt point of 48°C , as measured by DSC (**H-48**). Although this melt point is low for typical toner applications, it was studied because its melt transition occurs at a significantly lower temperature than the T_g of the primary toner polymer. This allows the crystallization behavior to be studied easily. A hyperbranched polymer with a melt point of 61°C was obtained by using a commercial mixture of C_{20} and C_{22} carboxylic acids for surface functionalization (**H-61**).

Linear crystalline polymers were included in this study for comparison. A polymer with approximately the same melting point (57°C) as the hyperbranched materials was synthesized from 1,6-hexanediol and adipic acid (**L-57**). Using this polymer in a toner reduces the minimum fusing temperature, but gives poor physical stability.⁹ A higher melt point linear polymer (116°C) was synthesized from 1,6-hexanediol and fumaric acid (**L-116**) and has been found to be useful in toner formulations.⁹

Blending of crystalline polymer with primary toner polymers was typically done by a low shear, batch melt mix process. The two polymers were heated to $175 - 190^{\circ}\text{C}$ in a glass round bottom flask. Agitation was sup-

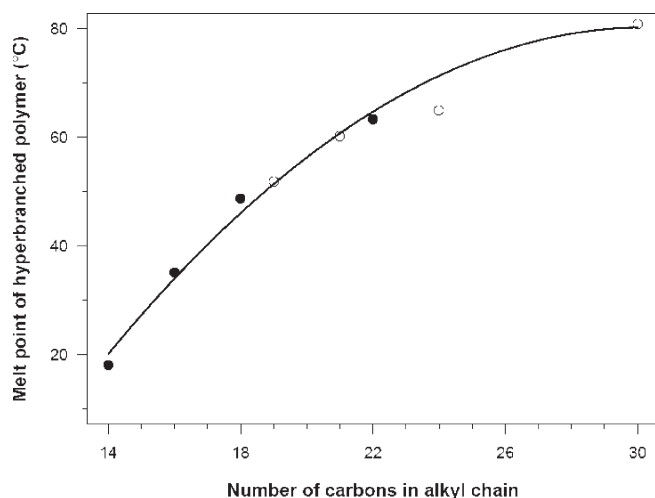


Figure 2. Melt point dependence of hyperbranched polymers on the chain length of surface group (● = monomers with $\geq 95\%$ purity; ○ = monomer blends).

plied from a half-moon impeller with the shaft speed set at 600 rpm. A Werner–Pfleiderer ZSK-30 twin-screw extruder was also used to blend the polymers. The barrel temperature of the zones was set at either 100 or 150°C and the effect of multiple passes through the unit was evaluated.

Crystallization

Thermal analysis of crystalline polymers and blends with primary toner polymers were performed using a modulated differential scanning calorimeter from TA Instruments (model 2920). The samples were heated to approximately 50°C above their melt point and then held for 5 minutes to insure complete melting. After this time the samples were cooled to 25°C at the desired cooling rate, which ranged from 1 to 10°C/minute. The non-isothermal exotherms were recorded for further analysis.

For a non-isothermal crystallization study, the energy released during crystallization is determined as a function of temperature. The relative crystallinity as a function of temperature T can then be formulated by using Eq. (1),

$$\theta(T) = \frac{\int_{T_c}^T (dH_c / dT) dT}{\Delta H_c} \quad (1)$$

where T_c is the temperature at which the onset of crystallization occurs, dH_c is the enthalpy of crystallization released during a small temperature range dT , and ΔH_c is the overall enthalpy of crystallization for the specific cooling condition studied.

For crystallization kinetics to be determined, the relative crystallinity must be expressed as a function of time. The relationship between the sample temperature and crystallization time t is given by

$$t = \frac{T_c - T}{\phi}, \quad (2)$$

where ϕ is the cooling rate.

The most common approach to describe the overall non-isothermal crystallization kinetics is the Avrami

TABLE I. Crystalline Parameters

Polymer	k_a ($\times 10^{-2}$, sec^{-1})	n	r_ϕ ($\times 10^{-2}$, sec^{-1})	X_c
H-48	5.98	1.20	8.11	0.87
H-61	4.04	1.34	5.31	0.86
L-57	2.77	2.72	3.17	0.79
L-116	2.04	2.18	2.42	0.91

model. This involves fitting the transformed data to the following equation,

$$\theta(t) = 1 - \exp[-(k_a \xi t)^n] \quad (3)$$

where k_a is the Avrami crystallization rate constant and n is a parameter that is influenced by the nucleation process and shape of the crystallites forming.¹⁰ The kinetic parameters were determined by fitting the transformed data to the model using a nonlinear curve fitting algorithm (Gauss–Newton).

The rate parameters determined by this approach are a function of the cooling rate used in the experiment. Therefore only relative comparisons, run under identical experimental conditions, are valid. It was observed that all four crystalline polymers had higher crystallization rates with faster cooling rates.

Another important measurement is the total amount of crystalline structure recovered after the material is heated above its melt point and then rapidly cooled. The extent of crystallization parameter X_c can be calculated by either comparing the total enthalpy of crystallization released during cooling with the first heating cycle, or, for polymer blends, comparing the cooling crystallization enthalpy with the theoretical value, which is estimated from the crystallization enthalpy of the pure crystalline polymer and its weight fraction in the blend.

To determine if the presence of a crystalline polymer leads to toner plasticization, the T_g of the polymer blend determined from a second heating cycle was compared with the T_g of the pure primary toner resin.

Rheology

Viscoelastic properties were measured using an ARES controlled stress dynamic mechanical analyzer and 25 mm parallel plates. Dynamic temperature scans were run from 80 to 200°C at 5°C/min using a measurement frequency of 6.28 radians/second. Frequency sweep measurements were made at various temperatures and covered the range of 0.1 to 100 radians/second.

Results and Discussion

Table I summarizes the estimated kinetic parameters and extent of crystallization for the four crystalline polymers. In this table, r_ϕ is the bulk rate of crystallization for a specific cooling condition. It is defined as the inverse of the time required for 50% of the crystal structure to form during cooling at a rate of 10°C/min. All four polymers crystallize rapidly during cooling and regain almost all of their crystalline structure by the time the samples reach room temperature. Although the linear polymers have a slower crystallization rate, all the rates are of the same order of magnitude.

A DSC scan for a polymer blend containing 10% of a crystalline hyperbranched polymer is shown in Fig. 3. On the initial and second heating cycle the melting point of the crystalline polymer T_m and glass transition temperature for the primary toner polymer T_g can be clearly observed. On the cooling cycle, a crystalliza-

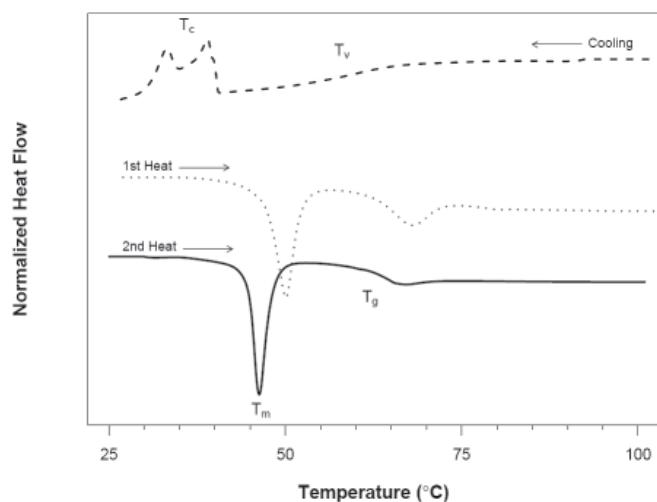


Figure 3. DSC thermogram of polymer blend containing 10% H-48 hyperbranched polymer.

TABLE II. Crystallization Parameters with Different Primary Toner Polymers

H-48 (wt %)	Primary Polymer	k_a ($\times 10^{-2}$, sec^{-1})	n	r_0 ($\times 10^{-2}$, sec^{-1})
5	P1	2.66	2.01	3.20
	P2	2.44	1.94	2.95
	P3	2.51	1.57	3.17
10	P1	2.74	1.72	3.39
	P2	2.64	1.87	3.21
	P3	3.15	1.25	4.23

tion transition for the crystalline polymer T_c and the temperature of vitrification for the primary toner polymer T_v are evident.

Figure 4 shows how the crystallization rate for the two hyperbranched polymers is affected by the amount of the primary toner polymer. The change in rate is small but there does appear to be a trend that the crystalline polymer crystallizes slower at lower concentration. The deviation from ideal behavior is most likely due to the presence of the some linear portions present in the hyperbranched backbone. The amount of crystalline structure formed during cooling for these samples are similar to that of pure crystalline polymer, with approximately 90% of the crystalline structure recovered.

Table II shows crystallization rate data of the hyperbranched polymers when blended with primary toner polymers having different chemical structures. **P1** is a linear polymer based on the reaction of a bisphenol A diol and terephthalic acid. **P2** is a partially crosslinked polymer that contains approximately 10–15 % gel content. **P3** is a lightly branched polymer that does not contain any bisphenol A diol monomer. The crystallization rate of the hyperbranched polymer does not appear to be significantly affected by structural differences in the primary toner polymer.

The crystallization rate for the hyperbranched crystalline polymer decreases by approximately 20% when processed at 175°C for 5 hours in the presence of a primary toner polymer (Fig. 5). Most of the rate change occurs within the first few hours. This may be indicative of a slight dependence of the crystallization rate on the size of the dispersed crystalline domain. The effect of differ-

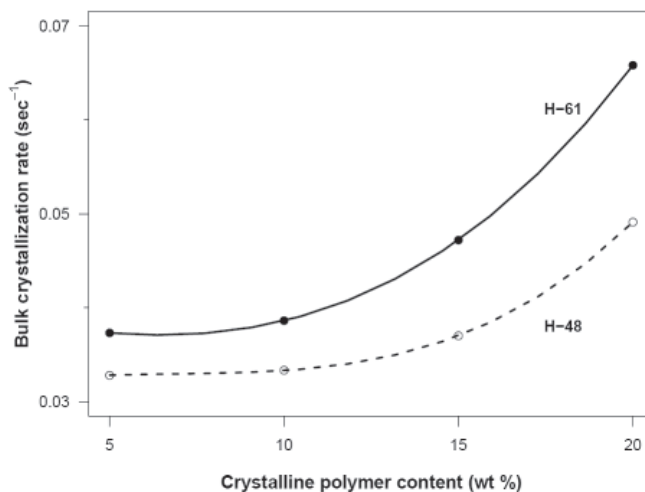


Figure 4. Crystallization rates for hyperbranched polymer blends.

TABLE III. Crystallization Parameters for Extruder Study

H-48 (wt %)	Temp. (°C)	N_p	k_a ($\times 10^{-2}$, sec^{-1})	n	r_0 ($\times 10^{-2}$, sec^{-1})
5	100	1	2.48	2.09	2.96
		3	2.44	1.94	2.95
	150	1	2.73	1.92	3.30
		3	2.63	2.00	3.16
10	100	1	2.70	1.83	3.30
		3	2.64	1.87	3.21
	150	1	2.88	1.82	3.52
		3	2.90	1.68	3.61

ent extruder processing conditions is shown in Table III. The number of passes through the extruder, N_p , does not appear to have any influence on the crystallization rate of these materials. Increasing the temperature used for blending appears to increase the rate, but only by 5 – 10%. This may indicate that more efficient dispersion occurs with lower extruder zone temperatures.

In contrast to the hyperbranched polymers, linear polymers show no tendency to crystallize upon cooling when blended with a primary toner polymer. Isothermal DSC experiments were attempted in which the enthalpy was monitored after the sample was cooled to room temperature. The higher melt point linear polymer showed an onset of crystallization after approximately 90 minutes, but proceeded very slowly. Quantitative rate information could not be obtained, but it is estimated that this polymer would require at least several days to regain a significant portion of its crystal structure. The lower melt linear polymer did not show any evidence of crystallization after 2 weeks.

Figure 6 shows the effect of the crystalline polymers on the T_g of the primary toner polymer. Hyperbranched polymers do not plasticize the primary toner resin even when incorporated at up to 20 weight percent. For these blends, the melt transition for the crystalline polymers can be clearly observed during multiple heating and cooling cycles. In contrast, the linear polymers dramatically decrease the T_g of the primary toner polymer and the melt transition of the crystalline polymer can only be observed during the initial heating cycle.

The behavior of the storage modulus of blends of containing 10% of the higher melting linear and hyper-

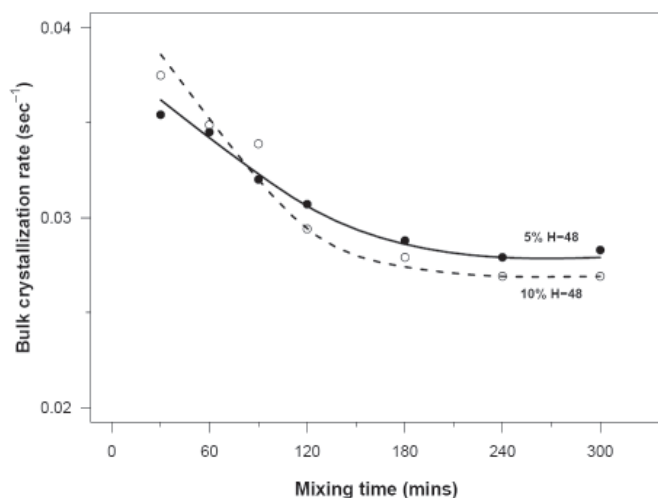


Figure 5. Influence of mixing time on crystallization rate.

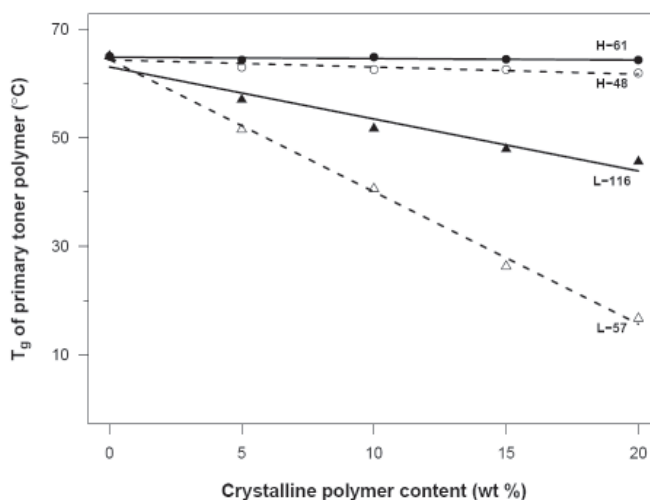


Figure 6. Plasticization of primary toner polymer.

branched crystalline polymers is shown in Fig. 7. The linear polymer decreases the storage modulus at low temperature, which is desirable for improving fusing properties. However, at higher temperature, the storage modulus is also reduced and therefore the hot offset temperature of the toner would be expected to decrease.

The hyperbranched polymer also decreases the storage modulus at low temperature and decreases the temperature at which the material begins to flow. At high temperature, the storage modulus is increased, which leads to a more desirable modulus-temperature relationship.

Conclusions

Hyperbranched polymers with crystalline surface groups crystallize rapidly and their crystallization rates are relatively unaffected by the presence of different primary toner polyesters. Blends containing hyperbranched polymers have a lower storage modulus and viscosity at low temperature, but increased storage modulus at higher temperatures.

Crystalline hyperbranched polymers should be useful in toner formulations to decrease the minimum fusing temperature without compromising storage stability or decreasing hot offset temperature.

References

1. E. Shirai, K. Aoki and M. Maruta, "The effect to the toner of various properties of the crystalline polyester", *Proc. IS&T's NIP 19: International Conference on Digital Printing Technologies*, (IS&T, Springfield, VA, 2003), pp. 119–122.
2. M. Serizawa, K. Daimon, H. Humano, Y. Ishihara, N. Fukushima and T. Imai, US Patent 6,607,864 (2004).
3. M. Aoki, M. Inoue, Y. Mikuriya and M. Hagi, US Patent 6,503,679 (2003).
4. K. Hayashi, M. Koyama, M. Uchida, H. Yamzaki and T. Uchida, US Patent 6,395,442 (2002).

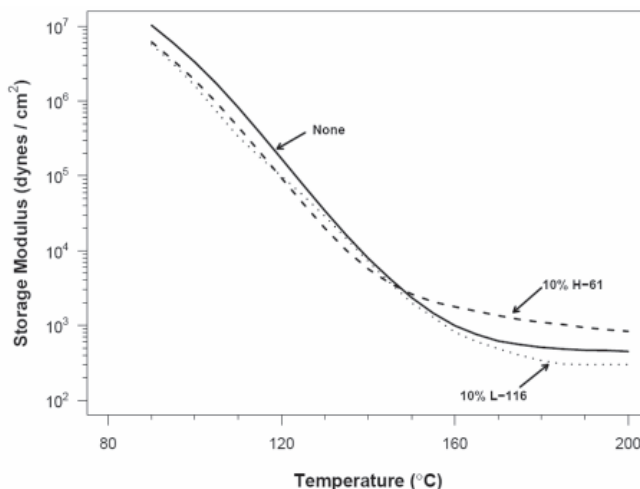


Figure 7. Storage modulus for primary toner polymer and blends.

5. P. Alexandrovich, J. Derimaggio and J. Wilson, US Patent 5,082,883 (1992).
6. E. Shirai, K. Aoki and M. Maruta, "The toner for low energy fusing by using crystalline polyester", *Proc. IS&T's NIP 17: International Conference on Digital Printing Technologies*, (IS&T, Springfield, VA, 2001), pp. 354–357.
7. E. Malmstrom, M. Johansson and A. Hult, *Macromol. Chem. Phys.*, **197**, 3199–3207 (1996).
8. E. Malmstrom, M. Johansson and A. Hult, *Macromol.*, **28**, 1698 (1995).
9. K. Aoki, Y. Fukushima, Y. Kanamaru and K. Akiyama, US Patent 6,383,705 (2002).
10. P. C. Hiemenz, *Polymer Chemistry*, (Merrel Dekker Inc., New York, 1984).